

Characteristics of Dusts Encountered during the Production of Cemented Tungsten Carbides

Aleksandr B. STEFANIAK^{1*}, Gregory A. DAY¹, Christopher J. HARVEY¹,
Stephen S. LEONARD², Diane E. SCHWEGLER-BERRY², Steve J. CHIPERA³,
Nancy M. SAHAKIAN¹ and William P. CHISHOLM²

¹Division of Respiratory Disease Studies, National Institute for Occupational Safety and Health, Morgantown, West Virginia 26505, USA

²Health Effects Laboratory Division, National Institute for Occupational Safety and Health, Morgantown, West Virginia 26505, USA

³Earth and Environmental Sciences Division, Los Alamos National Laboratory, Los Alamos, New Mexico 87545, USA

Received April 11, 2007 and accepted August 13, 2007

Abstract: Inhalation of cobalt (Co) and tungsten carbide (WC) particles, but not Co or WC alone, may cause hard metal disease, risk of which does not appear to be uniform across cemented tungsten carbide (CTC) production processes. Inhalation of Co alone or in the presence of WC may cause asthma. Hypothesizing that aerosol size, chemical content, heterogeneity, and constituent compaction may be important exposure factors, we characterized aerosols from representative CTC manufacturing processes. Six work areas were sampled to characterize aerosol size distributions (dust, Co) and 12 work areas were sampled to characterize physicochemical properties (using scanning electron microscopy with energy dispersive x-ray spectrometry [SEM-EDX]). Bulk feedstock and process-generated powders were characterized with SEM-EDX and x-ray diffraction. The dust mass median diameter was respirable and the cobalt respirable mass fraction was highest (37%) in grinding. Morphology of particles changed with processing: individual, agglomerate, or aggregates (pre-sintered materials), then mostly compacted particles (subsequent to sintering). Elemental composition of particles became increasingly heterogeneous: mostly discrete Co or W particles (prior to spray drying), then heterogeneous W/Co particles (subsequent work areas). Variability in aerosol respirability and chemical heterogeneity could translate into differences in toxicity and support detailed characterization of physicochemical properties during exposure assessments.

Key words: Hard metals, Asthma, Tungsten carbide, Cobalt, Aerosol particle physicochemical properties

Introduction

Exposure to aerosol generated during the manufacture of cemented tungsten carbides (CTC) can cause hard metal disease (HMD), an interstitial lung disease characterized by the presence of “bizarre” multinucleated giant cells in the lung interstitium, or occupational asthma (OA). Epidemiologic studies of cemented carbide workers have not consistently agreed on which work processes confer higher-risk of HMD or OA. Meyer-Bisch *et*

*al.*¹⁾ determined that employees who handled pre-sintered material (powder mixers, pressers, and shapers) were high-risk groups for the development of HMD, whereas Sprince *et al.*²⁾ determined that grinders who handled sintered CTC were a high-risk group. Occupational asthma has been reported among employees who handle feedstock powders and among sinterers and grinders^{1, 3)}. Toxicologists hypothesize that the presence of both cobalt (Co) and tungsten carbide (WC) particles in the lung are necessary to cause HMD via generation of reactive oxygen species (ROS)^{4–6)}. A clear toxicological mechanism for OA among cemented carbide workers is lacking⁷⁾;

*To whom correspondence should be addressed.

however, ionic Co (from particles containing Co either alone or in the presence of WC) may conjugate with proteins to form a hapten^{3, 8)}.

Much attention has been given to microanalytical characterization of particles in lung tissue or lung biopsy specimens of former and deceased CTC workers^{9, 10)}. Results of these studies often identified tungsten-containing particles in samples, but little or no Co, ostensibly due to the relatively higher solubility of Co in biological fluids¹¹⁾. In contrast, few surveys have reported the physicochemical characteristics of aerosols to which employees were exposed during the manufacture of CTC. Koponen *et al.*¹²⁾ and Kusaka *et al.*¹³⁾ reported that airborne particles generated during grinding were respirable multi-constituent W/Co particles. Other investigators analyzed particles collected in multiple work areas and determined that their chemical composition changed from discrete WC and Co particles in powder mixing to multi-constituent particles in pressing, forming, and grinding work areas^{14, 15)}.

Recently, the U.S. National Institute for Occupational Safety and Health (NIOSH) responded to a confidential employee request to perform a health hazard evaluation at a company that produces CTC blanks. This request presented a unique opportunity to build upon previous CTC aerosol characterization studies. The purposes of our study were to better understand production process influence on the: 1) size distribution of aerosols generated during the manufacture of CTC; 2) physicochemical properties of aerosol particles generated in 12 work areas that span the manufacture of CTC (from production of feedstock powders through finishing of sintered product); and 3) morphology and chemistry of bulk powders encountered during the production of CTC.

Materials and Methods

Cemented tungsten carbide (CTC) manufacturing process

Cemented tungsten carbide refers to a class of carbides that contain 80–95% WC bound in a matrix of 5–20% Co binder, with miscellaneous additives to impart performance-specific properties. Figure 1 is a schematic of the CTC manufacturing process at the company under study; asterisks denote the source of particles and powders studied. The process begins with separation of tungsten-containing scrap (from metalworking fluid sludge, etc.) to formulate ammonium paratungstate (APT) crystals. APT crystals are calcined (heat-treated) to form tungsten oxide, which is reduced in a hydrogen atmosphere to tungsten metal powder. Tungsten metal and carbon black are milled followed by carburization (heat treatment) to form WC powder. The WC powder is mixed with reclaimed powder (from sintered scrap), Co binder, and additives

(including nickel, chromium, titanium carbide, tantalum carbide, and vanadium) in accordance with customer specifications. Each powder formulation is suspended in solvent, milled, and dispersed in a spray dryer. By this process, the company produces several hundred different powder formulations. Powders are screened to achieve a customer-specified sizes, are quality checked, and are sent for compacting into “green” compacts (i.e., unsintered forms) by pneumatic pressing and extruding. Some green compacts may first be rough machined and all compacts are sintered (heat-treated in vacuum furnaces) to form CTC. During sintering, the compacts shrink, necessitating grinding to precise final dimension and finishing (sandblasting). Finished products are sent for quality testing before being shipped to customers.

Sample collection and analysis

1) Evaluation of airborne particle size distributions

Our first aim was to understand process influence on size distributions of airborne dust and cobalt-containing particles in six representative work areas: scrap reclamation, powder mixing, spray drying, screening, pressing, and grinding. For this aim, 10-stage multi-orifice uniform deposit impactor (MOUDI) samplers (Model 110, MSP Corp, Shoreview, MN) operated at 30 l min⁻¹ for 1 to 15 h were positioned with the inlet near breathing-zone height to sample general work area air. The 50% aerodynamic cutoff diameters (D_{50}) for the MOUDI samplers were >18, 10, 5.6, 3.2, 1.8, 1.0, 0.56, 0.32, 0.18, 0.10, 0.056, and <0.056 μm for the inlet, stages 1 to 10, and the final filter, respectively. A total of 11 samples were collected on pre-weighed polyvinyl chloride (PVC) substrate; prior to weighing, all substrate except the final filter were sprayed with silicone (Product No. 07041, MSP Corp) to minimize particle bounce during sampling.

The mass of airborne dust collected on each PVC substrate was determined gravimetrically using a calibrated microbalance (Model UMX2, Mettler Toledo Inc., Columbus, OH) stationed in a temperature- (21°C) and relative humidity- (50%) controlled chamber. After post-weighing, all substrates were submitted to a commercial laboratory for analysis of Co content in accordance with NIOSH Method 7300: Inductively Coupled Plasma-Atomic Emission Spectroscopy¹⁶⁾ (analytical limit of detection [LOD]=0.2 $\mu\text{g Co/filter}$; analytical limit of quantification [LOQ]=0.6 $\mu\text{g Co/filter}$).

The mass concentration and size distribution of dust and cobalt-containing particles in air were estimated for each MOUDI sample. In addition, the respirable mass fractions of dust and cobalt-containing particles were calculated for each sample. Estimates of the size distribution (mass median aerodynamic diameter [MMAD] and geometric standard deviation [GSD]) of dust and cobalt-

containing particles were calculated using methods described by Hinds¹⁷). The respirable mass fraction of particles was calculated by summing the average respirable fractions per impactor stage¹⁷) using the American Conference of Governmental Industrial Hygienists (ACGIH) respirable dust criteria¹⁸). Respirable particles were defined as particles having aerodynamic diameter $<10\text{ }\mu\text{m}$, with D_{50} of $4\text{ }\mu\text{m}$ ¹⁸). For the purposes of calculating the size distributions and respirable mass fractions of cobalt-containing particles, a mass value below the analytical LOD was assigned a value equal to the LOD.

2) Evaluation of airborne particle physicochemical properties

Our second aim was to investigate production process influence on particle physicochemical properties (morphology, elemental chemistry). The role of particle morphology, if any, in development of HMD or OA is unclear; however, morphology provides a visual indicator of differences in particle physical properties, which could be indicative of differences in chemical properties. Additionally, fiber-shaped whiskers may be generated during reduction of tungsten oxide, but it is unknown whether this morphology could contribute to HMD or pose a yet unidentified inhalation hazard¹⁹). Sixteen samples were collected from 12 different work areas (denoted by asterisks in Fig. 1), each representative of processes encountered in the CTC manufacturing industry and where changes in particle physicochemical properties were likely to occur because of processing conditions (e.g., heating, mixing, use of a solvent). Samples were collected using 10-stage MOUDI samplers positioned near the point of process operation and at breathing-zone height, operated at 30 l min^{-1} for 2 to 4 h. (Of the 16 samples, four were collected in the scrap reclamation work area.) Because each stage of the MOUDI sampler rotates during sample collection, particles were uniformly deposited on the substrate, thereby increasing the likelihood of obtaining a representative aerosol sample suitable for electron microscopy characterization. Additionally, use of a size-selective sampler permitted us to evaluate changes in particle morphology and chemistry as a function of aerodynamic size. Sampling durations and locations were selected based on results of the size-selective sampling data collected to address our first aim; D_{50} were >18 , 10, 5.6, 3.2, 1.8, 1.0, 0.56, 0.32, 0.18, 0.10, 0.056, and $<0.056\text{ }\mu\text{m}$ for the inlet, stages 1 to 10, and the final filter, respectively. The company processed several different powder formulations for varying amounts of time during the week in which samples were collected.

All 16 samples were collected on mixed cellulose ester (MCE) substrate, facilitating analysis of particle mor-

phology and elemental chemistry by scanning electron microscopy (SEM). To minimize the potential for particle contamination with silicon, a known constituent of abrasive grinding wheels, only the stage 1 substrate of each sampler was sprayed to reduce particle bounce. Particles collected on stage 1 ($D_{50}=10\text{ }\mu\text{m}$), stage 3 ($D_{50}=3.2\text{ }\mu\text{m}$), and stage 5 ($D_{50}=1.0\text{ }\mu\text{m}$) were characterized for each sample. The three particle sizes chosen for analysis are capable of penetrating into the respiratory tract^{18, 20}); all three are likely to be biologically relevant for OA, a disease of the pulmonary airways. Particle sizes that collect on stage 3 and stage 5 are capable of penetrating into the alveolar region of the lung^{18, 20}); these sizes are likely to be biologically relevant for HMD, a disease of the pulmonary interstitium. A section of each MCE filter was placed particle side up on double-stick carbon tape on an aluminum stub and sputter coated with gold/palladium (SPI Supplies, West Chester, PA).

All samples were analyzed at NIOSH using SEM (Model JEM6400, JEOL, Tokyo, Japan) and energy dispersive x-ray spectrometry (EDX, IMIX Microanalysis System, Princeton-Gamma Tech, Princeton, NJ). Secondary electron images and corresponding EDX spectra were obtained for over 1,250 particles. EDX spectra were collected from individual particles; when particles were agglomerated or aggregated, the spectra were separately collected from each component particle. Note that at least 25 particles per filter and three size fractions per sample were obtained, for a total of at least 75 particles per sample. The exceptions to this SEM analysis protocol were for the MOUDI stage 5 computer-controlled pressing sample and the stage 5 sintering sample, where fewer than 25 particles were located in several random fields. To ensure that the imaged object was an airborne particle that deposited on the MCE substrate and not an artifact of the substrate, the elemental constituents of each imaged particle were qualitatively identified using EDX analysis; "particles" having a spectrum of only carbon were not included in the data analysis, resulting in a net total of 1,262 workplace-sampled particles with corresponding elemental spectra. The accelerating voltage (20 kV) was held constant for all microscopic observations; magnification values ranged from 400 to 20,000. For identification of chemical constituents, the counting time was 30 s and the counting rate was between 2,000 and 3,000 counts per second.

3) Evaluation of bulk powder physicochemical properties

Bulk powder samples were collected from containers of feed-stock powders (tungsten metal, WC, and Co), pre-sintered powder discharged from a spray dryer, and from a dust collector connected to a chamfer grinder (used for final machining of post-sintered CTC products). These

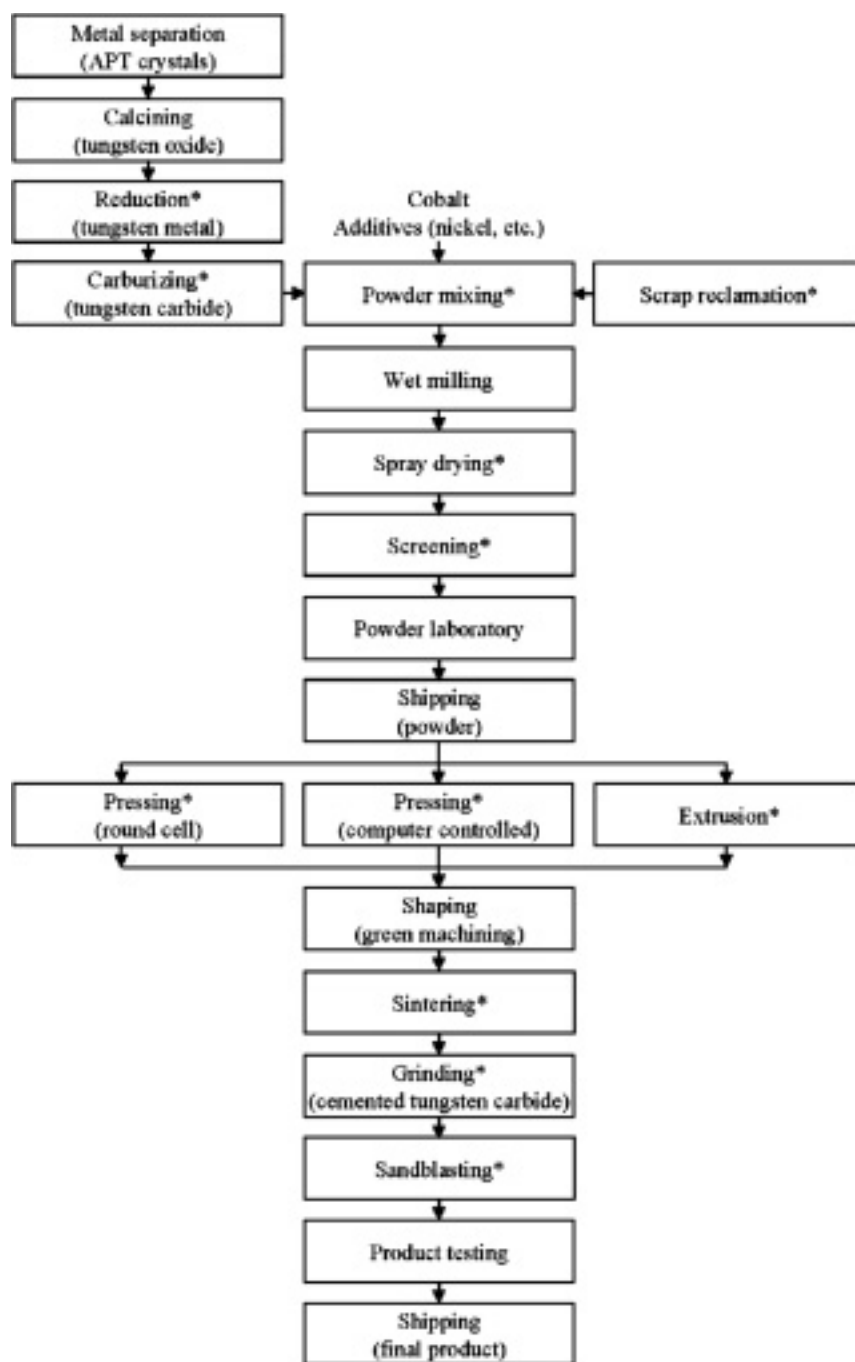


Fig. 1. Cemented tungsten carbide manufacturing process. Asterisks indicate the 12 work areas sampled to characterize aerosol physicochemical properties.

powders were collected from some of the same work areas where airborne particles were sampled and represented the spectrum of powders used in the manufacture of CTC at this company.

All bulk powder samples were analyzed at Los Alamos National Laboratory using SEM-EDX and powder x-ray diffraction (XRD). Each bulk powder sample was homogenized by riffing (repeatedly turning the container end-over-end then side-to-side) in a standard manner

and a sample was obtained for determination of particle morphology and identification of elemental constituents using SEM (Model XL20, Philips Electron Optics, Eindhoven, Netherlands) with an EDX detector (Model XL20, EDAX, Mahwah, NJ). The identity and relative abundance of crystalline constituents were determined using powder XRD (Siemens Model D500, Bruker AXS, Inc., Madison, WI).

For SEM-EDX analysis, a sample of each powder was

suspended in isopropyl alcohol and then subjected to ultrasonic agitation for several seconds to suspend particles. An aliquot of suspension was pipetted onto an aluminum stub and allowed to dry for several hours before being coated with carbon by vapor deposition. Secondary electron images were acquired using an accelerating voltage of 20 kV; magnification values ranged from 1,600 to 26,000. For bulk powder particles, the EDX spectra were collected from individual particles and in the case of agglomerate or aggregate particles, spectra were collected from each component particle separately. For identification of chemical constituents, the counting time was 15 s and the counting rate was approximately 2,000 counts per second.

XRD samples were mounted in a shallow titanium metal cavity or as a smear on an off-axis-cut quartz plate and run from 2 to 140° 2 θ overnight to ensure adequate counting statistics. The identity of constituents was determined by comparing diffraction patterns to reference patterns in the Inorganic Crystal Structure Database²¹. Relative abundances of crystalline phases were obtained from Rietveld²² and full-pattern fitting methods²³.

Results

Airborne particle mass concentrations and size distributions

As summarized in Table 1, airborne dust concentrations were variable among work areas, ranging from 128 $\mu\text{g}/\text{m}^3$

(dry grinding) to 4,031 $\mu\text{g}/\text{m}^3$ (powder mixing). Concentrations of cobalt varied among work areas by a factor of nearly 200; levels were lowest in grinding and highest in scrap reclamation and powder handling work areas. Figure 2 is a representative log-probability plot of cobalt mass data, illustrating that lognormal distributions were observed for all samples, except those designated in Table 1. As summarized in Table 1, airborne dust in the scrap reclamation, powder mixing, and spray drying work areas primarily consisted of non-respirable particles (MMAD >4 μm); in the grinding work area, dust particles were respirable (MMAD <4 μm). The MMAD of

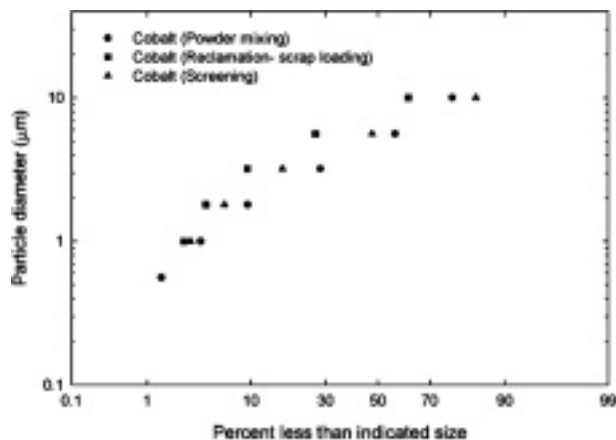


Fig. 2. Representative log-probability plots of cobalt mass data from the powder mixing, scrap reclamation, and screening work areas.

Table 1. Mass concentrations and size distributions of dust and cobalt-containing particles generated during the manufacture of cemented tungsten carbides (n=1 sample per work area)

Work area	Details	Total dust				Cobalt-containing particles			
		Conc. ($\mu\text{g}/\text{m}^3$)	MMAD ^a (μm)	GSD ^b	Resp Mass ^c (%)	Conc. ($\mu\text{g}/\text{m}^3$)	MMAD (μm)	GSD	Resp Mass ^c (%)
Scrap reclamation	Scrap loading	3,433	15	4	13	192	17	3	9
Scrap reclamation	Large crusher	1,817	14	4	15	64	>18 ^d	4	12
Scrap reclamation	Small crusher	555	10	5	25	21	16	4	12
Scrap reclamation	Ball mill	2,827	>18 ^d	4	9	132	>18 ^d	3	7
Powder mixing	Near charger	4,031	9	5	27	145	11	3	14
Powder mixing	Near charger	922	7	4	29	70	9	3	21
Spray drying	Near dryer	143	8	6	27	9	13	3	13
Screening	Next to screener	1,898	— ^e	—	43	81	10	2	15
Pressing	Inside press	472	— ^e	—	56	13	>18 ^d	4	14
Grinding	Dry grinder	128	2	4	52	1	6	4	37
Grinding	Next to grinder	229	3	4	48	1	7	3	34

^a MMAD is mass median aerodynamic diameter.

^b GSD is geometric standard deviation.

^c Resp Mass is respirable mass fraction of cobalt-containing particles calculated for each sample by summing the average respirable fraction per impactor stage¹⁷ using the ACGIH respirable dust criteria¹⁸.

^d Greater than 50% of the measured mass of analyte was on the initial stage of the impactor (i.e., greater than 18 μm aerodynamic diameter), precluding calculation of an exact value for the MMAD.

^e Aerosol distribution was bimodal, precluding calculation of a single estimate of the MMAD for the distribution.

airborne Co-containing particles was $>4\ \mu\text{m}$ in the scrap reclamation, powder mixing, spray drying, screening, pressing, and grinding work areas. MMADs for airborne dust and cobalt tended to be smaller in the grinding work area relative to other work areas. Among all samples collected, the respirable mass fraction of dust ranged from 9% (scrap reclamation- ball mill) to approximately 50% (pressing and grinding). Similarly, the respirable mass fraction of cobalt-containing particles ranged from 7% (scrap reclamation-ball mill) to 37% (grinding).

Airborne particle physicochemical properties

The morphology of airborne particles collected in representative work areas that span the CTC production process (reduction furnace, carburization furnace, powder mixing, spray drying, and grinding) are summarized in Fig. 3. Among work areas, there was no consistent distinctive shape for the particles, e.g., evidence of sharp-edged crystals. Within each work area, the morphology of airborne particles was similar among the three analyzed aerodynamic size fractions. Among work areas, the morphology of airborne particles varied with processing (see Fig. 3). In work areas that prepare and handle feedstock powders, airborne particles were isometric particles (see Figs. 3a(A) and 3c(A)), smaller isometric particles attached to the surface of larger irregular-shaped particles (see Fig. 3b(A)), or platelet-shaped particles (see Fig. 3d(A)). Airborne particles generated in the pressing and extrusion work areas were mostly round particles and/or compacted particles (data not shown). In the grinding work area (and sintering and sandblasting work areas), airborne particles had irregular-edges and appeared to be more compacted than feedstock materials (see Fig. 3e(A)). Fiber-shaped particles were not observed in any analyzed filter sections.

Elemental constituents of individual airborne particles collected from 12 work areas became increasingly heterogeneous as manufacturing proceeded from production of feedstock powders through finished CTC product. Within each work area, the elemental constituents identified in particles were generally similar among the three analyzed aerodynamic particle size fractions. (Carbon, a component of both the collection substrate and several metal carbides used in the production process, and oxygen were identified in nearly all particles.) Aerosols generated in work areas that prepared or handled feedstock powders (i.e., autoredution furnace, carburizing, and powder mixing) were generally homogeneous particles. Nearly all particles characterized from the autoredution furnace work area were elemental tungsten particles (Fig. 4a); only a few particles contained metal additives (cobalt, chromium, nickel, and titanium) or impurities such as calcium, iron, manganese, and silicon. Particles from the

carburizing work area were predominantly tungsten particles; some particles contained the same additives and impurities identified in particles sampled from the reduction work area. In the powder mixing work area, particles were almost exclusively Co; a few were W/Co particles or particles that contained metal additives such as nickel, tantalum, and titanium. In contrast to the homogeneous feedstock powders, aerosols generated in spray drying were elemental Co particles and multi-constituent W/Co particles; some W/Co particles contained the same impurities and additives identified in the precursor powders (Fig. 4b). Airborne particles in screening (Fig. 4c) and all other downstream work areas (e.g., grinding, as shown in Fig. 4d) were predominantly multi-constituent W/Co particles, with particles in each work area containing varying additive metals and impurities (see inset EDX spectra in Figs. 4c and 4d) consistent with those identified in the feedstock powders. (Aerosols generated during reclamation of sintered scrap materials were a mixture of elemental W particles and multi-constituent W/Co particles; some W/Co particles contained the same additives and impurities identified in the precursor powders.)

Bulk powder physicochemical properties

The morphology of each bulk powder is illustrated in Fig. 3. In general, the morphology of bulk powders was similar to the airborne particles collected in the work areas from which the bulks were obtained. The chemical constituents identified in bulk powders are summarized in Table 2. Feedstock powders were high purity, whereas powders from the spray dryer and the chamfer grinder were multi-constituent particles.

Discussion

Airborne particles

In general, process-dependent differences in total dust and cobalt concentrations were observed during the manufacture of cemented carbides. Airborne dust and cobalt concentrations were highest in work areas that handled powders (scrap reclamation, powder mixing, screening, and pressing) and lower in the work areas that finished solid CTC pieces (grinding). Relative to published historical exposure data^{13–15}, levels of airborne dust and cobalt in the powder mixing, pressing, and grinding work areas at this company were low. The MMAD of dust observed in the grinding work area (2 to 3 μm) is consistent with an MMAD of 2.8 μm reported in a Japanese CTC grinding facility¹³. The largest MMAD Co particle sizes were observed in the scrap reclamation and pressing work areas, consistent with operations such as mechanical crushing of solid pieces or compacting of powders. Smaller MMAD particle sizes were observed

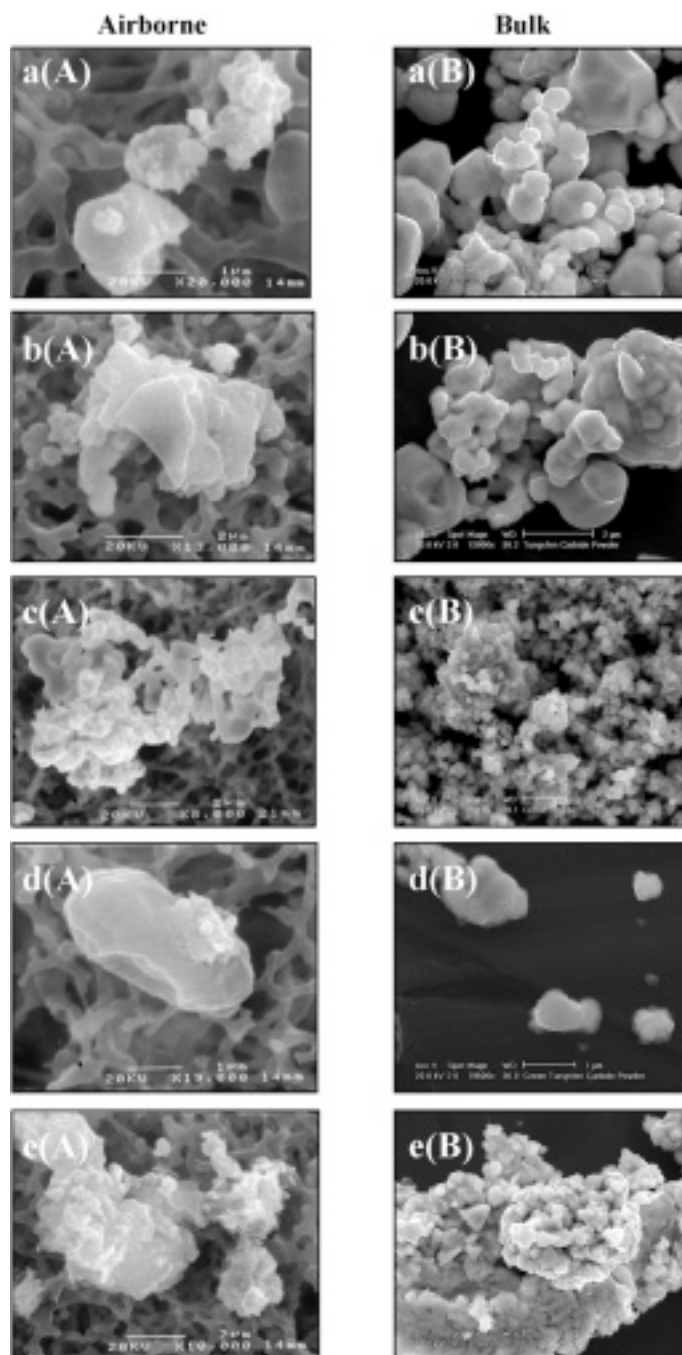


Fig. 3. Morphology of work-area sampled airborne (A) particles (collected on stage 3 of the micro-orifice uniform deposit impactor) and analogous bulk (B) powder materials. Particles shown are from: a(A) reduction furnace work area/ a(B) bulk tungsten metal powder; b(A) carburization furnace work area/ b(B) bulk tungsten carbide powder; c(A) powder mixing work area/ c(B) bulk cobalt powder; d(A) spray drying work area/ d(B) bulk powder from spray dryer; and e(A) grinding work area/ e(B) bulk chamfer grinder powder.

in the grinding work area, consistent with a high-energy, abrasive input activity. Consistent with the smaller MMAD values, the respirable mass fraction of dust (50%) and cobalt-containing particles (35%) was highest in the

grinding work area. Kusaka *et al.*¹³⁾ reported that 70% of Co in grinding facilities was associated with “respirable” particles (defined in that report as having aerodynamic size $<7 \mu\text{m}$). This factor of two difference in

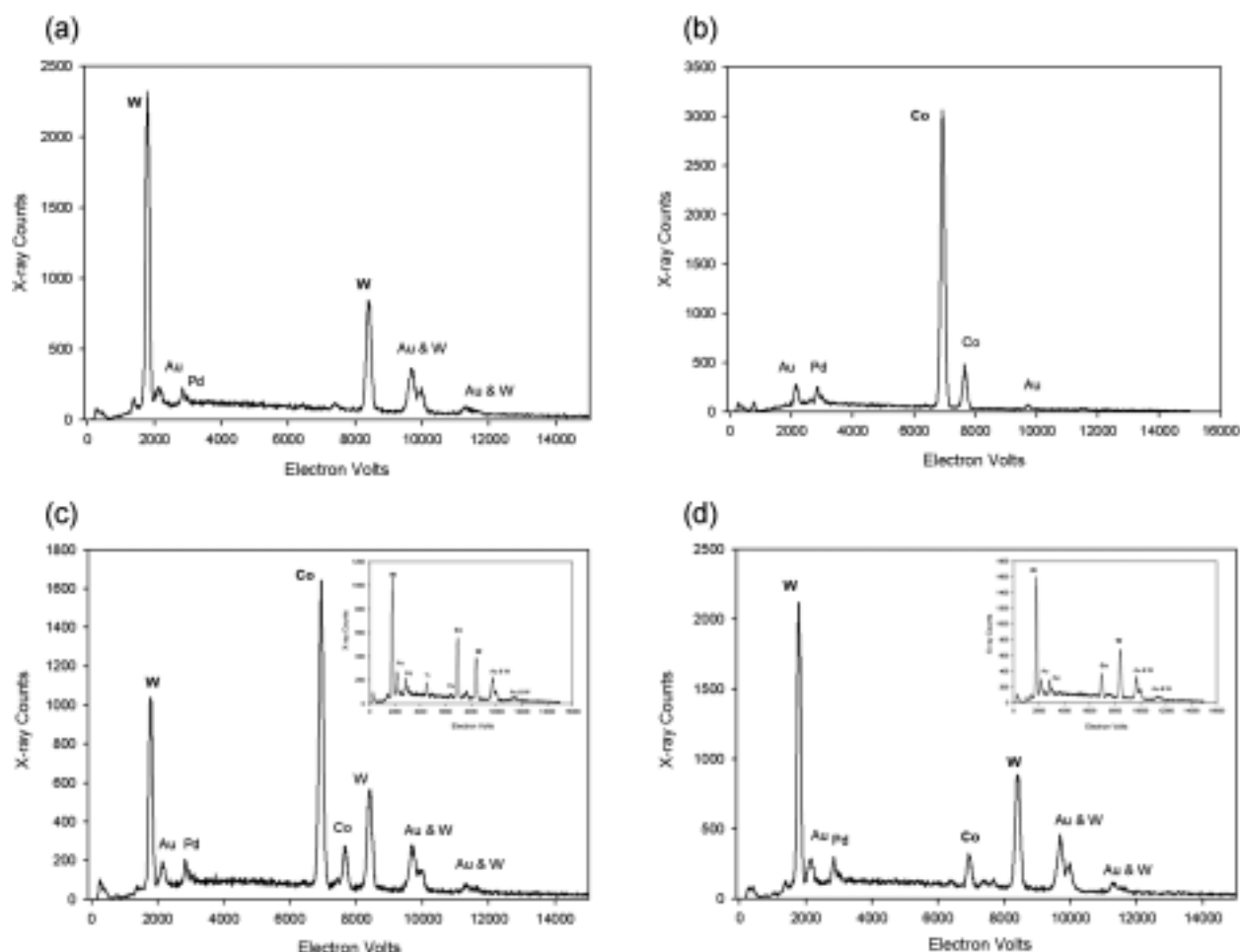


Fig. 4. Representative energy dispersive x-ray spectrometry spectra illustrating the increasing heterogeneity of elemental constituents of airborne particles generated during the manufacture of cemented tungsten carbide: (a) autoreduction furnace work area; (b) spray drying work area; (c) screening work area; and (d) grinding work area. Inset spectra in 3c and 3d illustrate metal additives or impurities identified in some particles in each work area. The gold and palladium peaks are from the sputter coating on the samples and are not constituents of the particles.

Table 2. Elemental and crystalline constituents of bulk powders samples

Powder	Constituents ^a	
	Elemental	Crystalline (relative abundance, %)
Tungsten metal	W	W (100%)
Tungsten carbide	W, C	WC (98.3%), W ₂ C (1.7%)
Cobalt	Co	Co (87%), Co ₃ O ₄ (13.1%)
Spray drying	W, C, Co	WC (82.6%), Co (11.8%), W (4.6%), W ₂ C (1.0%)
Chamfer grinder	W, C, Co	WC (84.7%), Co (11.2%), C (4.1%) ^b

^a W=tungsten metal, C=carbon, Co=cobalt, WC=tungsten carbide, W₂C=tungsten carbide, Co₃O₄=cobalt oxide.

^b Impure nature of material precluded definitive identification of the carbon-phase.

respirable mass fraction estimates between studies may partly be explained by differences in definitions of respirable (MMAD <4 μm versus <7 μm) and calculation methods- we weighted by the average respirable fraction

per impactor stage using the recently modified ACGIH respirable dust criteria¹⁸⁾, whereas Kusaka *et al.*¹³⁾ used an arithmetic summation of the mass of cobalt on each impactor stage.

Note that among all MOUDI sample filters, assignment of a mass value equal to the LOD for non-detectable cobalt masses was only necessary for a few filters from impactor stages having submicrometer size aerodynamic diameter cutoffs $<0.56\ \mu\text{m}$ (i.e., stage 6 and higher). For the purposes of calculating size distributions, the tails of the distribution on the log-probability plots were not weighted equally with the central 20 to 80% of the distribution¹⁷). As such, these substituted values did not contribute appreciably to the calculated size distributions. For the purposes of calculating respirable mass fractions, submicrometer size particles have higher probability of depositing in the alveolar region of the lung than do large particle sizes¹⁸). Thus, estimates of the respirable mass fraction could be sensitive to the choice of mass value substituted for censored data. In the current study, we substituted non-detectable masses with a value equal to the LOD. With the exception of the samples from the pressing and grinding operations, if non-detectable masses had been substituted with a value equal to the LOD divided by two or if the non-detectable values had been excluded from calculation of respirable mass fractions, our estimates would have decreased by less than 10% of the value reported in Table 1; for the samples collected in the pressing and grinding work areas, estimates of the respirable mass fractions would have been a maximum of 40% lower than reported in Table 1.

Assessment of particle binding forces can not be made directly using electron microscopy; however, process knowledge coupled with electron microscopy can be used to speculate on the nature of particle binding forces. The morphology of airborne particles in work areas that prepare and handle feedstock powders could be aggregate particles (defined here as particles held together by chemical or physical bonds) or agglomerate particles (defined here as particles held together by weak van der Waals forces or electrostatic bonds). For example, in the carburization work area, carbon powder and tungsten metal powder were heated in a furnace to form WC, which could have aggregate morphology because the energy imparted on the powders was sufficient to form chemical or physical bonds (see Fig. 3b(A)). In the powder mixing work area, Co powder was manually transferred to a drum that contained WC powder, which could form agglomerate particles, but not likely aggregate particles because of the low energy associated with this operation (see Fig. 3c(A)). In the pressing and extrusion work areas, airborne particles could be a mixture of agglomerate particles from dispersed feedstock powder and/or aggregate particles generated from pressed material (data not shown). In the sintering work area, pressed forms were heated to the melting temperature of Co in a furnace to form CTC (i.e., WC particles uniformly dispersed

in a Co matrix). Thus, in the grinding work area (and sintering and sandblasting work areas), airborne particles could have aggregate morphology because the energy imparted by the operation was sufficient to form chemical or physical bonds (see Fig. 3e(A)). In contrast to preliminary findings by Sahle *et al.*¹⁹) in the Swedish cemented carbides industry, fiber-shaped whiskers were not identified in our samples; however, our data do not exclude the possibility that tungsten-containing fibers exist in low frequencies at the company we studied or may be produced under other operating conditions elsewhere in the cemented carbides industry. We used MOUDI samplers to collect airborne particles, whereas a 25-mm diameter conductive cassette sampler such as that used to sample for asbestos fibers may be more appropriate for tungsten fibers¹⁶).

If Co particles in the presence of WC particles cause HMD via generation of ROS⁴⁻⁶), then our characterization of airborne particles may help to explain the inconsistent findings of epidemiological studies, e.g., between Meyer-Bisch *et al.*¹) and Sprince *et al.*²); only Sprince *et al.*²) showed a higher risk in the later stages of the CTC manufacturing process. We observed that airborne particles potentially available for inhalation in spray drying and all subsequent work areas were a mixture of elemental tungsten and elemental Co particles and/or multi-constituent W/Co particles (ostensibly WC/Co particles, but the relative carbon contribution of the collection substrate and metal carbides is unknown). It is interesting to speculate on the potential implications of our results, which suggest more intimate contact between Co and WC in post-screened particles relative to pre-spray dried particles, for generation of ROS and risk of HMD. It has been reported that the Co constituent of pre-sintered WC/Co powder is oxidized in vitro, releasing electrons that are transferred to the surface of WC where atmospheric oxygen is reduced, resulting in generation of ROS⁴⁻⁶). In pre-sintered powder, metallic Co and WC may be held in contact by weak electrostatic bonds or by van der Waals forces. In contrast, WC becomes physically bound in a Co matrix during sintering. Because of this greater proximity of metallic Co to WC in post-sintered alloy material, the ROS-generating capacity, and therefore hazard potential of post-sintered particles for HMD could be greater than that of pre-sintered powder.

Occupational asthma has been reported among employees who handle feedstock powders and among sinterers and grinders^{1, 3}). If exposure to Co, either alone or in the presence of WC, is sufficient to cause OA^{3, 8}), then our identification of Co in aerosols generated in the powder mixing and all downstream work areas may help to understand these epidemiological observations.

Despite the simultaneous processing of several differ-

ent powder formulations during sample collection, our results contribute to a better understanding of characteristics of aerosol particles generated during the manufacture of CTC. Because WC and Co powders are used in all powder formulations (only the ratio and the presence of additive metals may differ), the identities of elements comprising airborne particles are expected to be representative of this manufacturing facility. Our SEM-EDX results were consistent with previous studies^{14, 15} that reported differences in the chemical composition of airborne particles among powder mixing, pressing, forming, and grinding work areas and with reports^{12, 13} that airborne particles generated during CTC grinding were respirable multi-constituent WC/Co particles.

Bulk powders

The morphology and chemical composition of the bulk feedstock and spray dryer materials were consistent with properties of pre-sintered WC, Co, and WC/Co powders known to generate ROS⁶. Bulk powder physicochemical properties differed between feedstock and formulated powders. Feedstock powders were homogeneous powders, while spray dryer and chamfer grinder powders were multi-constituent materials with composition consistent with the basic formulation of CTC (80–95% WC, 5–20% Co).

Bulk feedstock powders consisted of smooth, mostly spherical isometric particles as shown in Figs. 3a(B) through 3d(B). Post-sintered bulk powder from the chamfer grinder consisted of particles that were also somewhat round, but relatively more compacted, than precursor or pre-sintered materials, as illustrated by the flattened face of the large aggregate particle shown in Fig. 3e(B). The basic morphology and elemental constituents of each bulk powder were qualitatively similar to the airborne particles collected in the work areas from which the bulks were obtained. Although minor additive metals such as nickel, chromium, titanium carbide, tantalum carbide, and vanadium were sometimes identified in airborne particles, the properties of the bulk powders were qualitatively similar to airborne particles.

Summary

We observed that the sizes of Co-containing aerosols generated during the production of CTC were highly variable, with MMADs ranging from 6 to >18 μm by work area. Among all work areas, airborne particle chemistry became more heterogeneous as manufacturing proceeded from preparation of feedstock powders through finishing of sintered product. In the context of the current toxicological hypotheses for HMD and OA, detailed characterization of airborne particle physicochemical properties may be warranted when performing exposure assessments

in the CTC industry.

Acknowledgements

The authors thank R. Boylstein at NIOSH for assistance with air sampling, and M. Fittipaldo at LANL for performing SEM analyses of the bulk powders. We also thank M. Hoover at NIOSH for useful discussion of this work, L. Millecchia, C. Piacitelli, and M. Keane at NIOSH for critical review of this manuscript, N. Edwards at NIOSH for data management and graphics development, and R. Scripsick at LANL for financial support with the XRD analyses and for useful discussion of this work. The authors declare that they have no competing interests, financial or otherwise.

References

- 1) Meyer-Bisch C, Pham QT, Mur J-M, Massin N, Moulin JJ, Teculescu D, Carton B, Pierre F, Baruthio F (1989) Respiratory hazards in hard metal workers: a cross sectional study. *Br J Ind Med* **46**, 302–9.
- 2) Sprince NL, Oliver LC, Eisen EA, Greene RE, Chamberlin RI (1988) Cobalt exposure and lung disease in tungsten carbide production. *Am Rev Respir Dis* **138**, 1220–6.
- 3) Shirakawa T, Kusaka Y, Fujimura N, Goto S, Kato M, Heki S, Morimoto K (1989) Occupational asthma from cobalt sensitivity in workers exposed to hard metal dust. *Chest* **95**, 29–37.
- 4) Lison D, Lauwery R, Demedts M, Nemery B (1996) Experimental research into the pathogenesis of cobalt/hard metal lung disease. *Eur Respir J* **9**, 1024–8.
- 5) Lison D, Carbonnelle P, Mollo L, Lauwerys R, Fubini B (1995) Physicochemical mechanism of the interaction between cobalt metal and carbide particles to generate toxic activated oxygen species. *Chem Res Toxicol* **8**, 600–6.
- 6) Zanetti G, Fubini B (1997) Surface interactions between metallic cobalt and tungsten carbide particles as a primary cause of hard metal disease. *J Mater Chem* **7**, 1647–54.
- 7) Cirla A (1994) Cobalt-related asthma: clinical and immunological aspects. *Sci Total Environ* **150**, 85–94.
- 8) Shirakawa T, Kusaka Y, Fujimura N, Goto S, Morimoto K (1988) The existence of specific antibodies to cobalt in hard metal asthma. *Clin Allergy* **18**, 451–60.
- 9) Rüttner JR, Spycher MA, Stolkin I (1987) Inorganic particulates in pneumoconiotic lungs of hard metal workers. *Br J Ind Med* **44**, 657–60.
- 10) Abraham JL, Burnett BR, Hunt A (1991) Development and use of a pneumoconiosis database of human pulmonary inorganic particulate in over 400 lungs. *Scanning Microsc* **5**, 95–108.
- 11) Edel J, Sabbioni E, Pietra R, Rossi A, Torre M, Rizzato G, Fraioli P (1990) Trace metal lung disease: in vitro

- interaction of hard metals with human lung and plasma components. *Sci Total Environ* **95**, 107–17.
- 12) Koponen M, Gustafsson T, Kalliomäki P-L, Kalliomäki K, Moilanen M (1981) Grinding dusts of alloyed steel and hard metal. *Ann Occup Hyg* **24**, 191–204.
 - 13) Kusaka Y, Kumagai S, Kyono H, Kohyama N, Shirakawa T (1992) Determination of exposure to cobalt and nickel in the atmosphere in the hard metal industry. *Ann Occup Hyg* **36**, 497–507.
 - 14) Koponen M, Gustafsson T, Kalliomäki P-L (1982) Cobalt in hard metal manufacturing dusts. *Am Ind Hyg Assoc J* **43**, 645–51.
 - 15) Yamada Y, Kido T, Honda R, Ishizaki M, Tsuritani I, Yamaya H, Nogawa K (1987) Analysis of dusts and evaluation of dust exposure in a hard metal factory. *Ind Health* **25**, 1–10.
 - 16) National Institute for Occupational Safety and Health (1994) NIOSH Manual of Analytical Methods (NMAM®), 4th Ed., Schlecht PC and O'Connor PF (Eds.), 94–113 DHHS (NIOSH) Publication, Cincinnati.
 - 17) Hinds WC (1986) Data Analysis. In: Cascade impactor sampling and data analysis, Lodge JP and Chan TL (Eds.), 45–77, American Industrial Hygiene Association, Akron.
 - 18) Lippman M (1999) Rationale for particle size-selective aerosol sampling. In: Particle size-selective sampling for particulate air contaminants, Vincent JH (Ed.), 18, American Conference of Governmental Industrial Hygienists, Cincinnati.
 - 19) Sahle W, Laszlo I, Krantz S, Christensson B (1994) Airborne tungsten oxide whiskers in a hard-metal industry. Preliminary findings. *Ann Occup Hyg* **38**, 37–44.
 - 20) Stuart BO, Liroy PJ, Phalen RF (1986) Particle size-selective sampling in establishing threshold limit values. *Appl Occup Environ Hyg* **1**, 138–44.
 - 21) Inorganic Crystal Structure Database, Copyright 2003–2005 by Fachinformationszentrum (FIZ) Karlsruhe. <http://icsdweb.fiz-karlsruhe.de/index.php>. Accessed October 25, 2005.
 - 22) Bish DL, Howard SA (1988) Quantitative phase analysis using the Rietveld method. *J Appl Cryst* **21**, 86–91.
 - 23) Chipera SJ, Bish DL (2002) FULLPAT: A full-pattern quantitative analysis program for X-ray powder diffraction using measured and calculated patterns. *J Appl Cryst* **35**, 744–9.